LSTM Prediction Model based on Modified Bald Eagle Search for Offshore Wind Power

Yijing Chen *, Xiao Guo **‡, Jiulong Sun **, Chunhua Li *, Xiaojiang Guo *, Xu Sun *, Yanbo Che **

* China Huaneng Clean Energy Research Institute Technology Co., Ltd., Beijing, 102209, China

** Key Laboratory of Smart Grid of Education Ministry, Tianjin University, Tianjin 300072, China

(yijing.chen20@gmail.com, guo_xiao@tju.edu.cn, 2021234034@tju.edu.com, lchh_1990@126.com, 3064648381@qq.com, 1042236895@qq.com, ybche@163.com)

‡Corresponding Author; Xiao Guo, Key Laboratory of Smart Grid of Education Ministry, Tianjin University, Tianjin 300072, China, Tel: +86 13752483140, Fax: +86 13752483140, guo_xiao@tju.edu.cn

Received: 02.12.2023 Accepted:30.01.2024

Abstract- With the rapid development of new energy generation technology, a large number of wind distributed power supply into the power system. Accurate power load forecasting can effectively improve the consumption of wind power generation and realize the economic operation of the system. However, as the structure of the power system becomes more and more complex, it is difficult for traditional load forecasting methods to realize accurate prediction. In order to further improve the load prediction accuracy, this paper proposes a Long Short-Term Memory (LSTM) prediction model based on Modified Bald Eagle Search (MBES) algorithm. First, the LSTM prediction model is constructed and the fitness of the model is calculated based on the initialized parameters. Then, the parameters of the LSTM load prediction model are optimized by the proposed MBES. Finally, the load prediction is carried out under the optimal location parameters. Simulation examples show that the proposed model and algorithm have higher prediction accuracy.

Keywords Model predictive control, interconnected data centers, multiple time scales optimal scheduling, distributed power supply, LSTM.

1. Introduction

In the current landscape of global energy development, confronting deep-rooted challenges such as resource scarcity and low utilization efficiency necessitates an imminent energy transition [1, 2]. As new energy installed capacity continues to rise, China is confronted with increasingly conspicuous energy consumption issues, resulting in annual economic losses reaching tens of billions of dollars due to the "three abandoned" problem. The precision of load forecasting holds the potential to empower power grid companies in devising more economical and low-carbon planning and scheduling programs. This, in turn, facilitates the enhancement of new energy consumption while concurrently reducing overall system costs. Thus, the significance of accurate load forecasting becomes paramount in optimizing energy dispatch and addressing the challenges posed by the "Three Abandonments."

Two primary approaches currently dominate power load forecasting: one relies on mathematical statistical modeling algorithms [3, 4], while the other hinges on machine learning algorithms [5-7]. Mathematical statistical models offer computational simplicity, practicality, and versatility. However, in the case of complex nonlinear load data, the inherent lack of robustness in statistical algorithms poses a challenge, leading to significant prediction errors. In contrast, machine learning algorithms exhibit the capacity for more precise predictions. Nevertheless, traditional machine learning models suffer from the limitation of having fewer adjustable parameters. Given the vastness and complexity of contemporary power data, the inability to input a sufficient number of influential factor variables hampers the effective

expression of hidden information within the data, thereby impeding the attainment of accurate prediction results.

In recent years, the rapid advancement of artificial intelligence has led to the widespread application of deep learning algorithms, such as convolutional neural networks (CNN) [8, 9], recurrent neural networks (RNN) [10, 11], and LSTM [12, 13], in power load forecasting. These algorithms, known for their exceptional nonlinear mapping and adaptive capabilities, have yielded remarkable outcomes. Notably, LSTM has exhibited outstanding performance in addressing prolonged time series issues. A model for short-term load forecasting in power systems, integrating CNN and LSTM networks, is introduced in Ref. [14]. Through comparative analysis with existing methods, the proposed technique demonstrates superior precision and accuracy in short-term load forecasting. Another hybrid approach for power load forecasting is presented in Ref. [15], combining the Prophet and LSTM models. The Prophet model predicts linear and nonlinear data, while LSTM is employed to train the residuals associated with nonlinear data. Subsequently, the prediction data from Prophet and LSTM undergo joint training using Back Propagation Neural Network (BPNN), significantly enhancing prediction accuracy. Ref. [16] puts forth a novel hybrid model incorporating variational mode decomposition and long- and short-term memory, coupled with seasonal factor elimination and error correction. The efficacy and practicality of this hybrid model are substantiated through a comprehensive case study involving four real load datasets from both Singapore and the United States. The experimental results underscore the substantial improvement in prediction accuracy offered by the proposed model compared to existing counterparts.

In summary, LSTM network is a very effective deep learning method in short-term forecasting of electric load, but LSTM network will have the problem of hyper-parameter selection thus affecting the prediction accuracy. Therefore, this paper proposes the MBES-LSTM prediction model based on the improvement of the vulture search optimization algorithm. The main contributions and organization of this paper are as follows:

- Construct the LSTM prediction model and calculate the model fitness based on the initialized parameters.
- Optimizing the position change parameters in the selection search space stage of the vulture search optimization algorithm for the problem that it is easy to fall into local optimum.
- Optimize the parameters of the LSTM load forecasting model by the proposed MBES, and carry out load forecasting under the optimal location parameters.

It can be verified through the examples that the proposed model can effectively predict the hourly power load value, and can provide data for the future power generation plan of the grid, and the proposed algorithm has a higher prediction accuracy compared with other algorithms.

2. LSTM Networks

The LSTM network, a variant of the temporal recursive neural network, was proposed by Hochreiter and Schmidhuber in 1997 [17]. It was specifically designed to address persistent challenges encountered in general RNN. Over the years, LSTM has evolved into the predominant model for feature extraction in time series data and has found extensive application in power system load forecasting.

LSTM is a notable subtype of RNN, featuring a hidden layer comprising one or more memory units. Each unit is equipped with a forgetting gate, an input gate, and an output gate. The structural configuration is depicted in Fig. 1.

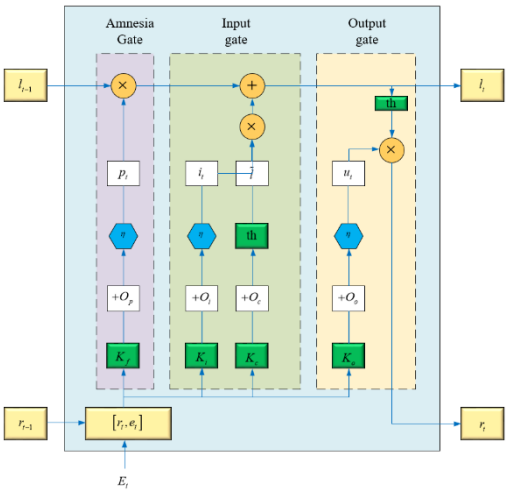

Fig. 1. LSTM structure diagram.

- Oblivion Gate: The oblivion gate p_t is tasked with overseeing the decision of whether the long-term state should persist. This determination is collectively influenced by the present moment, the input e_t, and the output r_{t-1} from the preceding moment, namely:

$$p_t = \eta\left(K_P \times [r_{t-1}, e_t] + O_P\right) \tag{1}$$

Where:

The forgetting gate is characterized by K_p, which represents the weighting matrix. O_p is attributed to the bias vector, and $\eta(\bullet)$ is indicative of the sigmoid activation function.

- Input gate: Its purpose is to set up a new unit state, labeled as $\tilde{\cdot}$, and in which the control of how much information to add and other processing, that is:

$$i_t = \eta\left(K_i \times [r_{t-1}, e_t] + O_i\right) \tag{2}$$

$$l_t = \tanh\left(K_c \times [r_{t-1}, e_t] + O_c\right) \tag{3}$$

Where: i_t corresponds to the output of the input gate; K_i is a weight matrix associated with the input gate; O_i signifies the input bias, serving as the initial point for the input; and $\tilde{\cdot}$

represents the current state of the input cell; K_c is a matrix of weights; O_c represents the bias associated with the cell state; the matrix $[r_{t-1}, e_t]$ consists of two vectors; (4) corresponds to the output from the preceding time step, and e_t serves as the input for the current time step; $\eta(\bullet)$ denotes the sigmoid activation, while $\mathrm{th}(\bullet)$ is characterized by a hyperbolic tangent function.

- Output Gate: Within the output gate, the output from the preceding moment r_{t-1} and the current moment e_t are conveyed through $\eta(\bullet)$ to p_t, as follows:

$$R_t = \eta\left(K_o \times [r_{t-1}, e_t] + O_o\right) \tag{4}$$

$$l_t = p_t \times l_{t-1} + i_t \times l_t \tag{5}$$

$$r_t = u_t \times \mathrm{th}(l_t) \tag{6}$$

Where: The weight matrix affiliated with the output gate is denoted by K_o, while the bias term linked to the output gate is indicated by O_o.

In the structure of the LSTM model, the distinctive three-gate architecture, coupled with the inclusion of hidden states possessing storage capabilities, enables the effective management of extended dependencies on historical data. First, the current hidden state l_t employs the forgetting gate to regulate the previous hidden state l_{t-1}. This regulatory mechanism is responsible for deciding which information from the previous state is to be discarded and which should be preserved. Subsequently, the architectural design discards particular details in the hidden state l_t and the forgetting gate, while introducing novel information through the input gate. Following a sequence of computations, the state l_t undergoes updates. Consequently, the LSTM utilizes the output gate, the cell state l_t, and the tanh layer to determine the final output value r_t.

3. Improving the Vulture Search Optimization Algorithm

3.1. Vulture Search Optimization Algorithm

The Bald Eagle Search (BES) optimization algorithm, a novel approach conceived by H.A. Alsattar in 2020, draws inspiration from the hunting strategies of the bald eagle. The bald eagle, a formidable raptor widely distributed across North America, is renowned for its robust physique and exceptional observational prowess [18].

In the quest for prey, a bald eagle adheres to a precise series of steps. Initially, it strategically identifies a search region determined by the concentration of prey populations and subsequently proceeds to soar towards that destination. Subsequently, the eagle conducts a thorough water search within the designated area, honing in on the most suitable prey. Finally, the eagle adeptly adjusts its flight altitude, executing a swift dive towards the water's surface, ensuring a successful capture.

The BES algorithm simulates this hunting behavior by breaking it down into three discrete phases: space selection, prey search, and swooping capture, illustrated in Fig. 2.

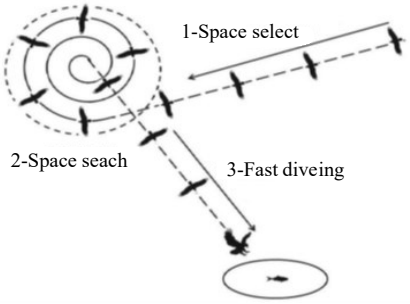

Fig. 2. Continuous hunting behavior of bald eagles during hunting.

3.1.1 Selection of search space

During the select search space phase, the bald eagle randomly designates a search region to locate the area with the highest prey concentration. The formula for updating the condor position in this phase is as follows:

$$Pos^i_{new} = Pos_{best} + \alpha \cdot rand(Pos_{mean} - Pos_i) \tag{7}$$

Where: Pos^i_{new} symbolizes the current location of the i-th bald eagle, while Pos_{best} indicates the optimal search position as ascertained through the ongoing exploration conducted by the bald eagles; α is the parameter governing the positional change; Pos_{mean} is a parameter controlling the variation in position, within the range of $(1.5, 2)$; *rand* represents a randomly generated number within the range of (0, 1); Pos_{mean} denotes the average distribution of bald eagle positions since the previous search; Pos_{mean} signifies the position of the i bald eagle.

3.1.2 Searching for space prey

In the spatial prey search phase, the bald eagle employs a distinctive spiral flight pattern to meticulously scan the designated search area in pursuit of optimal swooping positions for capturing prey.

The BES optimization algorithm utilizes an averaging approach for computing individual position updates in this stage. As the search points uniformly converge towards the central point, the averaged solution is utilized through the multiplication of the discrepancy between the current search position and the following point by the polar coordinate on the axis, resulting in the derivation of the new position point. Furthermore, this process encompasses the addition of the product obtained by multiplying the difference between the current position of the bald eagle and the search centre point by the polar coordinate on the axis, contributing to the determination of the refreshed search space. Concurrently, it

promotes exploration diversity, contributing to a more thorough exploration of the search area, i.e.:

$$\theta(i) = \beta \times \pi \times \text{rand}(0,1) \tag{8}$$

$$\theta(i) = \beta \times \pi \times \text{rand}(0,1) \tag{9}$$

$$m(i) = \theta(i) + \varsigma \times \text{rand}(0,1) \tag{10}$$

$$a \times m(i) = m(i) \times \sin\left[\phi(i)\right] \tag{11}$$

$$b \times m(i) = m(i) \times \cos\left[\phi(i)\right] \tag{12}$$

$$a(i) = \frac{a \times m(i)}{\max\left(\left|a \times m\right|\right)} \tag{13}$$

$$b(i) = \frac{b \times m(i)}{\max\left(\left|b \times m\right|\right)} \tag{14}$$

Where: $\phi(i)$ signifies the polar angle within the spiral equation; $m(i)$ denotes the polar diameter in the spiral equation; $\beta \in (0,5)$ and $\varsigma \in (0.5,2)$ function as variables influencing the trajectory of the spiral, whereas $a(i)$ and $b(i)$ denote the condor's position in polar coordinates, both assigned the value $(-1,1)$.

Therefore, the location of the bald eagle is updated below:

$$Pos_{new}^{i} = Pos^{i} + a(i) \times (Pos^{i} - Pos_{mean}) + b(i) \times (Pos^{i} - Pos^{i+1}) \tag{15}$$

Where: Pos^{i+1} denotes the subsequent updated location of the initial i bald eagle.

3.1.3 Diving to capture prey

When the vulture identifies its target, it promptly descends and advances toward the target from the optimal position. Leveraging the motion state during this phase, the polar coordinate equation can be formulated as follows:

$$Pos_{new}^{i} = \text{rand}(0,1) \times Pos_{best} + \delta_x + \delta_y \tag{16}$$

$$\delta_x = a1(i) \times (Pos^{i} - \lambda_1 \times Pos_{mean}), \lambda_1 \in [1,2] \tag{17}$$

$$\delta_y = b1(i) \times (P^{i} - \lambda_2 \times P_{mean}), \lambda_2 \in [1,2] \tag{18}$$

Where: λ_1 and λ_2 represent the best and center positions, respectively.

3.2. Improvement of Vulture Search Optimization Algorithm

The Modified Bald Eagle Search (MBES) optimization algorithm refines the parameter in Eq. (8) during the search space selection phase, transforming it from a constant value within $(1.5,2)$ to a dynamic range, as illustrated below:

$$u_t = \exp(\frac{T-t}{T}) - 1 \tag{19}$$

$$Pos_{new}^{i} = Pos_{best} + u_t \times m(Pos_{mean} - P^{i}) \tag{20}$$

Where: u_t represents the control parameter governing the condor's positional adjustment; t denotes the present iteration count; and T signifies the maximum iteration limit.

4. MBES-LSTM Prediction Model

4.1. MBES Algorithm Based Parameter Optimization

The LSTM model's key parameters are commonly determined based on scholars' experience, resulting in significant randomness and potentially unsatisfactory prediction accuracy, sometimes leading to issues of local optima. To address these challenges, we employ the MBES algorithm for optimizing the LSTM neural network. In the context of the MBES algorithm framework, the optimization objectives encompass the number of nodes in the hidden layer, learning rate, and regularization coefficient for the LSTM network. The optimization procedure for the model comprises four primary steps:

Step 1: Establish the LSTM network topology and initialize all pertinent parameters following Eqs. (1) to (6).

Step 2: Define the parameter search ranges based on randomly assigned values for the parameters under optimization.

Step 3: Compute the fitness value for each individual (referred to as a "bald eagle" in this context) using equation (15). The fitness value is indicative of the Root Mean Square Error (RMSE) observed in the model's validation dataset. If the computed fitness is globally minimal, it is designated as the best fitness for that instance, representing the optimal position of the "bald eagle". This value is then compared with the global best fitness; if it is lower, it is substituted.

Step 4: Commence iteration. Continuously update the three hyperparameters earmarked for optimization using the MBES algorithm and repeat steps 3-4 until the maximum iteration threshold is reached.

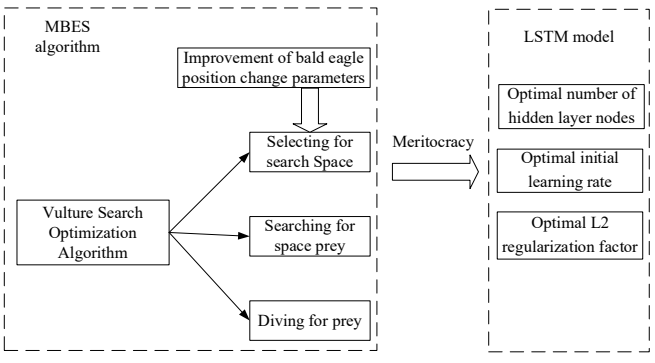

Fig. 3. Modeling flow of MBES-LSTM based power load forecasting.

Fig. 3 depicts the modeling flowchart. Beginning with the vulture search optimization algorithm, adjustments are made to the vulture position change control parameter to mitigate model over-parameterization. Next, the MBES algorithm is utilized to ascertain the optimal count of nodes in the hidden

layer, the initial learning rate, and the L2 regularization coefficient for the LSTM model. This broadens the search range of parameters to retain essential information. Subsequently, the refined parameters are applied for load prediction, yielding accurate results.

4.2. LSTM Prediction Model Based on MBES Algorithm

The flowchart in Fig. 4 illustrates the procedural steps of the MBES-LSTM prediction model:

Step 1: Initialize the parameters for LSTM (T_{iter}, P_R, P_1, P_2) and the MBES algorithm, which includes configuring the bald eagle population count N to be 5, setting a maximum iteration threshold M at 20, defining an upper boundary for parameter U_b, establishing a lower boundary for parameter L_b, specifying the number of dimensions D, and initializing the sample dataset.

Step 2: The fitness value for data generation during LSTM training is determined by the mean square error. This value is continuously updated in real-time as the input data is fed into the model. Equations (15), (16), and (20) are employed to calculate the position of the bald eagle within the iteration range. If the newly computed position is found to be more favorable, an update is applied to the existing position.

Step 3: Utilizing the optimal combination of parameters derived from the previous step, the LSTM model is employed to make predictions and generate corresponding output results.

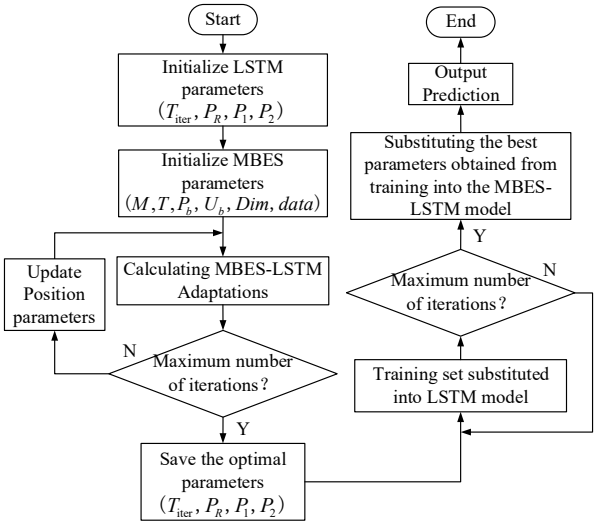

Fig. 4. Flowchart of the MBES-LSTM model prediction process.

5. Example Analysis

Electricity load data represents the aggregate demand for electrical energy within a specific region over a defined timeframe. The electric power load data employed in this chapter is sourced from the load forecasting data of the 2016 Mathematical Modeling Competition for Electricians, encompassing a city in northern China.

Originally utilized in the Load Forecasting Competition within the 2016 Mathematical Modeling Competition for Electricians, this dataset comprises information on electrical loads, temperatures, and humidity for a city located in the northern region of the country. The dataset spans from February 1, 2015 to May 7, 2015. For this chapter, data from February 1, 2015 to April 29, 2015 serves as the training set, while the hourly load data from April 30, 2015 is reserved for prediction testing.

During the initialization stage of LSTM parameters, the algorithm refines the optimal quantity of nodes in the hidden layer, the initial learning rate, and the coefficients for L2 regularization. Table 1 outlines the parameter settings for the MBES-LSTM model.

Table 1. LSTM model routine parameter settings

General Settings	MBES
Maximum number of iterations N=20	$\lambda_1 = 2, \lambda_2 = 2$
Population size P = 10	a=10
Number of variables to be optimized C = 3	R=1.5

Five common short-term electricity predictive models for load estimation are chosen for the purpose of comparison., including unoptimized LSTM, GWO (Grey Wolf Optimizer)-LSTM, PSO (Particle Swarm Optimizer)[19] -LSTM, FA (Firefly Algorithm)-LSTM and SSA[20] (Sparrow Search Algorithm)-LSTM. The initialization parameters of MBES comparison algorithms are shown in Table 2.

Table 2. Algorithm parameter settings

Arithmetic	Parameterization
PSO	Localized search capability V1=1
	Global search capability V2=2
GWO	M1=0.3
FA	Maximum attraction β = 2
	Light absorption intensity v=1
	Step factor = 0.2
SSA	Safety value ST = 0.6
	Discovery Proportion PD = 0.7
	Sparrow aware of danger SD = 0.2

As shown in Fig. 5, preprocessed electric load data is incorporated into each model and various algorithms are utilized to derive different load forecast curves.

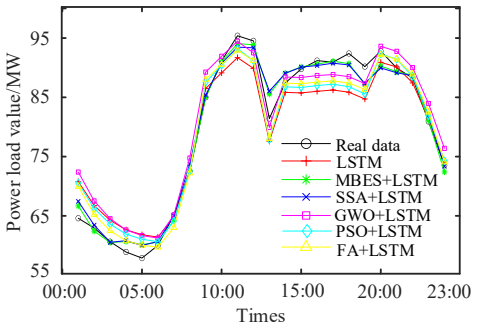

Fig. 5. Comparison of prediction results of different algorithms.

In Fig. 5, various curves illustrate different iterations of the LSTM forecasting model. Upon closer examination of these curves, it becomes evident that the MBES-LSTM model, when employed for load forecasting, demonstrates superior overall curve fitting performance compared to other algorithms. Although occasional minor deviations occur at specific points, the general trend favors the MBES-LSTM model. To provide a more in-depth analysis, subsequent sections will delve into error assessment.

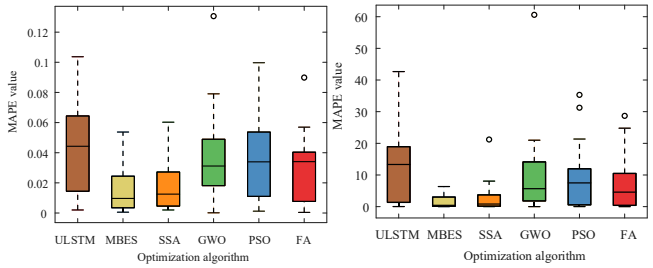

(a) MSE Box-Line Chart (b) RMSE Box-Line Chart

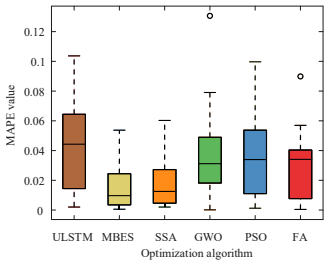

(c) MAPE box plots

Fig. 6. Error boxplots of the six prediction models.

Figure 6 demonstrates the effectiveness of the MBES algorithm as compared to the other five algorithms when employed on the dataset. This is showcased through box-and-whisker plots that illustrate the algorithm's performance across three key metrics: Mean Absolute Percentage Error (MAPE), Mean Squared Error (MSE), and Root Mean Squared Error (RMSE).

The boundaries of the box in the visual representation depict the upper quartile Q_3 and lower quartile Q_1 of the metric distribution. The terminal points of the upper and lower extensions of the box indicate the threshold values for outliers in the metric distribution, denoted as Q_3+1.5IQR and Q_1-1.5IQR , respectively. The parameter denoted by IQR=$Q_3 - Q_1$ signifies the width of the box. By analyzing the median value depicted in the boxplot and considering the width of the box, we can empirically assess the distribution of a specific indicator in the test set. A lower median value and a narrower box width indicate improved prediction accuracy and a more tightly concentrated distribution of prediction errors. As depicted in Figure 6, the integration of various algorithms with the LSTM prediction model for the test set results in a noticeable reduction in median values across three metrics, signifying an overall enhancement in average load prediction accuracy. Particularly noteworthy is the significant decrease in median values for all three metrics when combining the MBES and SSA algorithms with LSTM. Crucially, it is observed that the median and box width of the MBES algorithm consistently remain lower and narrower than those of the SSA algorithm. This observation suggests that, when combined with the LSTM model, the MBES algorithm achieves higher prediction accuracy.

Table 3. MSE, RMSE and MAPE values for several models in the test set

Estimation norm	MBES	SSA	GWO	FA	PSO
MSE	2.361	2.922	15.418	15.563	16.748
RMSE	1.537	1.709	3.927	3.945	4.093
MAPE	0.016	0.018	0.050	0.044	0.053

The average Mean Absolute Percentage Error (MAPE), Mean Squared Error (MSE), and Root Mean Squared Error (RMSE) values for different algorithms in the test set are summarized in Table 3. The table distinctly demonstrates a significant improvement in metrics for the MBES method compared to both the SSA algorithm and the other three methods. In particular, MBES exhibits reductions of 0.19% in MAPE, 0.1727% in RMSE, and 0.5606% in MSE when compared to the SSA algorithm. This emphasizes the superior performance of MBES in minimizing errors and enhancing predictive accuracy.

The error analysis chart in Fig. 7 illustrates the prediction errors of different algorithms at various time points, providing a comprehensive view of the accuracy of each algorithm throughout the entire prediction process. As depicted in the graph, although the proposed MBES-LSTM model exhibits occasional higher prediction errors at specific moments, its predictions remain more stable across all time points throughout the entire day compared to other algorithms.

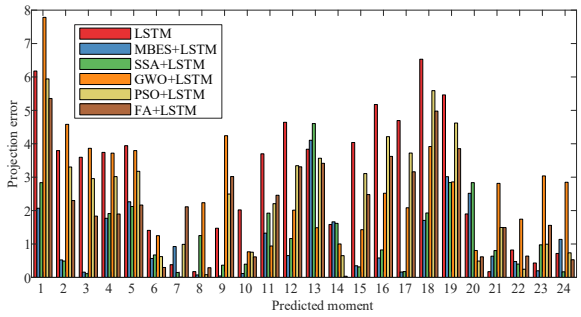

Fig. 7. Comparison of prediction errors at different moments.

Fig. 8 shows the R coefficient analysis plot of MBES algorithm and the four comparison algorithms, the regression value R represents the correlation between the predicted outputs and the target outputs, the closer the value of R is to 1 means that a stronger correlation between the predicted and output data leads to increased predictability, while a weaker correlation results in higher levels of randomness.

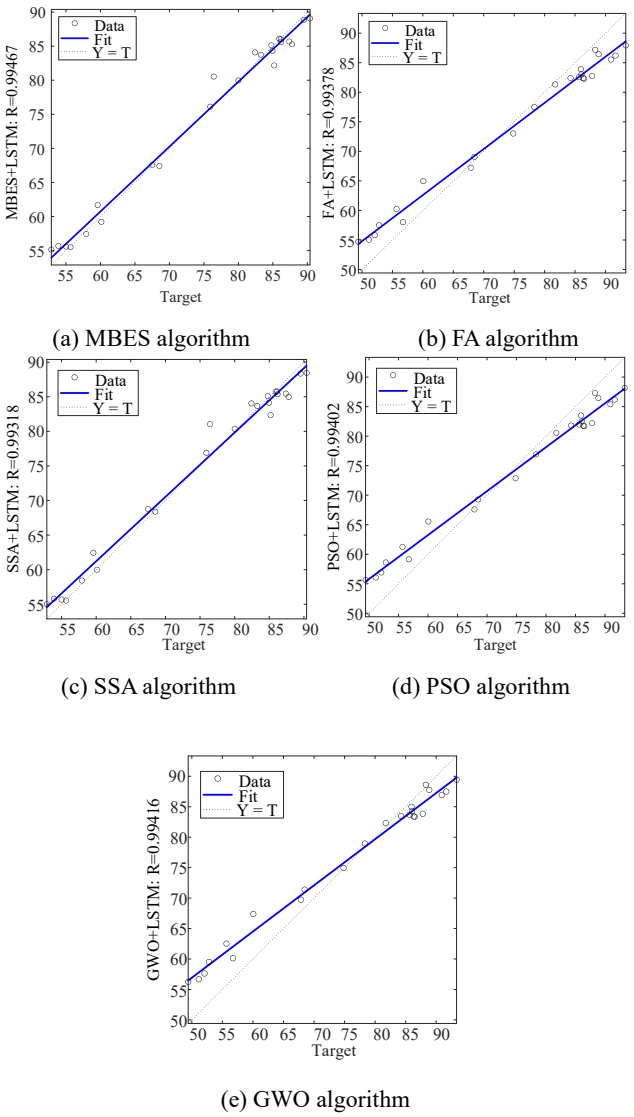

(a) MBES algorithm (b) FA algorithm

(c) SSA algorithm (d) PSO algorithm

(e) GWO algorithm

Fig. 8. R-coefficient analysis of different algorithms.

The coefficient analysis results of the MBES algorithm and four comparative algorithms are presented in Table 4. From the table, it is evident that the relationship between the predictive and output data for the MBES algorithm is more closely aligned compared to the comparative algorithms. This observation serves as evidence for the superior predictive performance of the MBES-LSTM model. The intricate connection observed in the analysis underscores the effectiveness of the MBES algorithm in accurately forecasting and generating output data. This supports the conclusion that the MBES-LSTM model exhibits a high level of prediction accuracy.

Table 4. Coefficient analysis results of MBES algorithm with four comparative algorithms

Arithmetic	R-factor
MBES	0.99467
SSA	0.99318
GWO	0.99416
FA	0.99378

6. Conclusion

In this paper, the MBES-LSTM prediction model is proposed based on the improvement of the vulture search optimization algorithm. Firstly, the LSTM load forecasting model is established, and the model's adaptability is calculated according to the initialized parameters. Then, the position change parameters in the selection search space stage are optimized for the problem that the vulture search optimization algorithm is easy to fall into local optimum. Finally, the parameters of the LSTM load forecasting model are optimized by the proposed MBES, and load forecasting is carried out under the optimal position parameters. The following conclusions are drawn through the validation of the arithmetic examples:

- The proposed MBES-LSTM model can effectively predict the hourly power load value and can provide data for the future power generation plan of the grid.
- Compared with other algorithms, the optimization of the parameters of the proposed MBES-LSTM load forecasting model can get better optimization results, which can effectively improve the load forecasting accuracy.

The MBES-LSTM prediction model achieves good prediction results and can provide powerful data support for the economic dispatch of power system. However, due to the influence of scenarios, data and other factors, its application scope and limitations exist, so the prediction accuracy of this prediction model is still to be improved. For short-term load forecasting, there are some issues that deserve further study in future research as follows:

Further expansion and refinement of the original data, this paper only considered the impact of the existing local average temperature, humidity, date type, etc. on the load, if the data of major festivals and complex meteorological factors can be collected, the accuracy of load forecasting will be further improved.

The scale and complexity of the power system will continue to expand with the continuous development of electric vehicles, drones, and renewable energy, and in the future, it will be necessary to dig deeper into the influencing factors and consider electricity loads that are more relevant to the actual situation in order to achieve better development.

Acknowledgement

This paper is supported by the National Key R&D Program of China(2023YFB4204700) and the CHNG science and technology project (HNKJ20-H54).

References

[1] P. K. Kushwaha and C. Bhattacharjee, “An Extensive Review of the Configurations, Modeling, Storage Technologies, Design Parameters, Sizing Methodologies, Energy Management, System Control, and Sensitivity Analysis Aspects of Hybrid Renewable Energy Systems,” Electric Power Components and Systems, vol. 51, no. 20, pp. 2603–2642, Dec. 2023, doi:

10.1080/15325008.2023.2210556.

[2] P. K. Kushwaha and C. Bhattacharjee, "Integrated techno-economic-environmental design of off-grid microgrid model for rural power supply in India," Journal of Information and Optimization Sciences, vol. 43, no. 1, pp. 37–54, Jan. 2022, doi: 10.1080/02522667.2022.2032557.

[3] J. F. Rendon-Sanchez and L. M. De Menezes, "Structural combination of seasonal exponential smoothing forecasts applied to load forecasting," European Journal of Operational Research, vol. 275, no. 3, pp. 916–924, Jun. 2019, doi: 10.1016/j.ejor.2018.12.013.

[4] S. Bae and A. Kwasinski, "Spatial and Temporal Model of Electric Vehicle Charging Demand," IEEE Trans. Smart Grid, vol. 3, no. 1, pp. 394–403, Mar. 2012, doi: 10.1109/TSG.2011.2159278.

[5] H. Mansoor, M. Shabbir, M. Y. Ali, H. Rauf, M. Khalid, and N. Arshad, "Spatio-Temporal Short Term Load Forecasting Using Graph Neural Networks," in 2023 12th International Conference on Renewable Energy Research and Applications (ICRERA), Oshawa, ON, Canada: IEEE, Aug. 2023, pp. 320–323. doi: 10.1109/ICRERA59003.2023.10269401.

[6] H. Bakiri, L. Massawe, H. Maziku, H. Ndyetabura, and N. Mvungi, "Design Requirements and Technical Architecture of a Fault- and Restoration-Based Load Forecasting Mechanism for Tanzania Secondary Distribution Electric Power Grid," in 2021 10th International Conference on Renewable Energy Research and Application (ICRERA), Istanbul, Turkey: IEEE, Sep. 2021, pp. 190–197. doi: 10.1109/ICRERA52334.2021.9598591.

[7] A. A. Mamun, M. Hoq, E. Hossain, and R. Bayindir, "A Hybrid Deep Learning Model with Evolutionary Algorithm for Short-Term Load Forecasting," in 2019 8th International Conference on Renewable Energy Research and Applications (ICRERA), Brasov, Romania: IEEE, Nov. 2019, pp. 886–891. doi: 10.1109/ICRERA47325.2019.8996550.

[8] W. H. Chung, Y. H. Gu, and S. J. Yoo, "District heater load forecasting based on machine learning and parallel CNN-LSTM attention," Energy, vol. 246, p. 123350, May 2022, doi: 10.1016/j.energy.2022.123350.

[9] S. Rafi, Nahid-Al-Masood, S. Deeba, and E. Hossain, "A Short-Term Load Forecasting Method Using Integrated CNN and LSTM Network," IEEE ACCESS, vol. 9, pp. 32436–32448, 2021, doi: 10.1109/ACCESS.2021.3060654.

[10] M. Xia, H. Shao, X. Ma, and C. W. De Silva, "A Stacked GRU-RNN-Based Approach for Predicting Renewable Energy and Electricity Load for Smart Grid Operation," IEEE Trans. Ind. Inf., vol. 17, no. 10, pp. 7050–7059, Oct. 2021, doi: 10.1109/TII.2021.3056867.

[11] F. Dewangan, A. Y. Abdelaziz, and M. Biswal, "Load Forecasting Models in Smart Grid Using Smart Meter Information: A Review," Energies, vol. 16, no. 3, p. 1404, Jan. 2023, doi: 10.3390/en16031404.

[12] I. Bodur, E. Celik, and N. Ozturk, "A Short-Term Load Demand Forecasting based on the Method of LSTM," in 2021 10th International Conference on Renewable Energy Research and Application (ICRERA), Istanbul, Turkey: IEEE, Sep. 2021, pp. 171–174. doi: 10.1109/ICRERA52334.2021.9598773.

[13] T. Inagata, Y. Mizuno, K. Matsunaga, F. Kurokawa, M. Tanaka, and N. Matsui, "A Forecasting Method of Peak-Cut of Power Demand Using LSTM at A Clinic," in 2023 12th International Conference on Renewable Energy Research and Applications (ICRERA), Oshawa, ON, Canada: IEEE, Aug. 2023, pp. 1–6. doi: 10.1109/ICRERA59003.2023.10269447.

[14] S. H. Rafi, Nahid-Al-Masood, S. R. Deeba, and E. Hossain, "A Short-Term Load Forecasting Method Using Integrated CNN and LSTM Network," IEEE Access, vol. 9, pp. 32436–32448, 2021, doi: 10.1109/ACCESS.2021.3060654.

[15] T. Bashir, C. Haoyong, M. F. Tahir, and Z. Liqiang, "Short term electricity load forecasting using hybrid prophet-LSTM model optimized by BPNN," Energy Reports, vol. 8, pp. 1678–1686, Nov. 2022, doi: 10.1016/j.egyr.2021.12.067.

[16] L. Lv, Z. Wu, J. Zhang, L. Zhang, Z. Tan, and Z. Tian, "A VMD and LSTM Based Hybrid Model of Load Forecasting for Power Grid Security," IEEE Trans. Ind. Inf., vol. 18, no. 9, pp. 6474–6482, Sep. 2022, doi: 10.1109/TII.2021.3130237.

[17] V. Shanmugapriya, Y. Rathod, and S. Vidyasagar, "Smart Energy Management for a Hybrid DC Microgrid Electric Vehicle Charging Station," International Journal of Renewable Energy Research, vol. 13, no. 3, pp. 1259–1276, 2023, doi: 10.20508/ijrer.v13i3.14143.g8798.

[18] A. Chhabra, A. G. Hussien, and F. A. Hashim, "Improved bald eagle search algorithm for global optimization and feature selection," Alexandria Engineering Journal, vol. 68, pp. 141–180, Apr. 2023, doi: 10.1016/j.aej.2022.12.045.

[19] P. K. Kushwaha, P. Ray, and C. Bhattacharjee, "Optimal Sizing of a Hybrid Renewable Energy System: A Socio-Techno-Economic-Environmental Perspective," Journal of Solar Energy Engineering, vol. 145, no. 3, p. 031003, Jun. 2023, doi: 10.1115/1.4055196.

[20] P. K. Kushwaha and C. Bhattacharjee, "Integrated techno-economic-enviro-socio design of the hybrid renewable energy system with suitable dispatch strategy for domestic and telecommunication load across India," Journal of Energy Storage, vol. 55, p. 105340, Nov. 2022, doi: 10.1016/j.est.2022.105340.